Electronic contribution to friction on GaAs

Yabing Qi [1,2], J. Y. Park [2], B. L. M. Hendriksen [2], D. F. Ogletree [2], and M. Salmeron [2,3]

[1] *Applied Science and Technology Graduate Group, University of California, Berkeley, California 94720, USA*

[2] *Materials Sciences Division, Lawrence Berkeley National Laboratory, University of California, Berkeley, California 94720, USA*

[3] *Department of Materials Sciences and Engineering, University of California, Berkeley, California 94720, USA*

(Dated: May 4, 2008)

Abstract

The electronic contribution to friction at semiconductor surfaces was investigated by using a Pt-coated tip with 50nm radius in an atomic force microscope sliding against an n-type GaAs(100) substrate. The GaAs surface was covered by an approximately 1 nm thick oxide layer. Charge accumulation or depletion was induced by the application of forward or reverse bias voltages. We observed a substantial increase in friction force in accumulation (forward bias) with respect to depletion (reverse bias). We propose a model based on the force exerted by the trapped charges that quantitatively explains the experimental observations of excess friction.

PACS numbers: 46.55.+d, 68.37.Ps, 73.40.Qv, 81.40.Pq

I. INTRODUCTION

Understanding and controlling friction are both scientifically interesting and technologically important.[1–5] Friction is the process of energy dissipation when the surfaces of two objects slide against each other. Atomic force microscopy (AFM) is an ideal tool in studying friction on the nanometer scale. In the elastic regime, when the AFM tip is brought into close proximity to a surface, the atoms in the topmost atomic layers are elastically displaced from their equilibrium positions under the applied load and lateral stress until a minimum energy configuration is reached. When the tip slides over the substrate, the inter-atomic distances of the interface atoms are first elastically modified and then relaxed back to equilibrium positions. One way that energy can be dissipated is by coupling of the atomic relaxations to phonon modes that propagate away from the contact. In insulators, this is the most important mechanism (in the elastic regime). In metals and semiconductors, there is an additional possibility of electronic contributions to the friction, for example by the creation of electron-hole pairs.[6–8]

Semiconductors offer an interesting platform to investigate the electronic contribution to energy dissipation. First of all, it is possible to reversibly the change carrier density near the surface by many orders of magnitude by applying an electric field across the contact. In addition, depending on the polarity of an applied bias voltage, the asymmetry in the potential distribution between accumulation and depletion allows us to test its influence on the friction. Recently, we studied the friction of silicon *pn* junctions covered with a thin oxide layer as a function of bias voltage and demonstrated a contribution to the friction force that depends on bias polarity: a substantial excess friction was detected in the heavily doped p region under a forward bias.[9,10] In this work, we show that this effect also occurs in n-type GaAs covered with a thin oxide layer, suggesting that it is, indeed, a general property of semiconductor materials.

II. EXPERIMENT

The sample was an n-type GaAs(100) substrate doped with tellurium to a concentration of $1.2 \times 10^{18}/cm^3$. After the cleaning procedure described in Ref.[11], the sample was etched in $1M$ HCl solution for 30 s and dried in a flow of dry nitrogen gas. A fresh oxide was

formed by subsequently dipping the GaAs sample in ultra pure water for 10 s. The oxide comprises a mixture of As_2O_3 and Ga_2O_3.[12] The presence of the oxide on the GaAs surface is important because it prevents irreversible tip-surface adhesion between the platinum coated AFM tip and the GaAs surface, which would otherwise lead to wear.[13] AFM topographic images in contact mode revealed that the oxide surface had a smooth amorphous morphology with a root-mean-square roughness of 2.3 Å . To determine the oxide layer thickness, the sample was characterized by x-ray photoelectron spectroscopy (XPS) by using Al $K\alpha$ x-ray in a PHI-5400 system before and after etching. Figure 1 shows the As 2p spectral region before and after the etching procedure. Two peaks can be clearly identified corresponding to oxidized and non-oxidized arsenic at binding energies of 1325.7 and 1322.6eV, respectively. These values are approximately 1 eV lower than those reported by Vilar et al.[14] for a semi-insulating GaAs(100) sample (1326.1 and 1323.8 eV, respectively). A possible cause of the lower binding energies is the high doping level in our GaAs substrate, which brings the Fermi level closer to the conduction band level. The ratio between the peak areas of the oxidized and non-oxidized species is significantly reduced by etching, changing from 2.80 to 1.76 after the etching. The oxide thickness is calculated to be 10 Å according to Ref.[14].

After etching, within 10 min of preparation, the sample was transferred to an RHK STM/AFM system[15] in an ultrahigh vacuum chamber with a base pressure in the 10^{-9} torr range for the friction experiments.[16,17] It is necessary to perform the experiments in vacuum to prevent electrochemical oxidation at the water meniscus formed around the tip apex in humid air that can mask other bias-induced effects.[18,19]

We used cantilevers with nominal spring constants of 3 N/m coated with approximately 5 nm of chromium (adhesion layer) and 15 nm of platinum.[20] The normal force was kept constant during imaging, while the current and the friction force were simultaneously recorded. The sample was mounted on a metallic sample holder and Ohmic contact was established by gently scratching the back of the sample and applying a thin layer of indium gallium eutectic between the sample and the holder. The bias was applied to the sample holder. The values of the applied load used in this study were sufficiently small to prevent wear of the oxide surface. Although some tip wear was observed, no sample wear traces were observed in subsequent high-resolution images, and the friction and adhesion measurements were reproducible.

To determine the forces, the cantilever spring constant was calibrated by using the

resonance-damping method of Sader et al.,[21] while the lateral force was calibrated with the wedge method of Ogletree et al.[22] The radii of the metal-coated tips were 15-30 nm before contact, as measured by a scanning electron microscope (Zeiss Gemini Ultra-55). When measured after a contact experiment, the radii were found to be 45-60 nm. Since the measured friction force did not vary at a constant total load ($< 50\,nN$) and did not show a time-dependent behavior in the elastic regime, we assumed that the changes in the tip radius took place soon after the first contact, with minimal changes during subsequent contact measurements. The fact that we could measure the current during the entire experiment indicates the presence of conductive layers at the tip apex. We suppose that the Pt layer was partially deformed upon the contact measurement, but a continuous Pt layer is still present at the tip apex, permitting us to measure a stable current. The total load is the sum of the applied load and the absolute value of the adhesion force (determined from force-distance measurements).

III. RESULTS

Figure 2(a) shows a friction map (gray scale: bright, high friction; dark, low friction) as a function of the applied load at a 0V sample bias. In this experiment, the friction force is measured while the tip is scanning back and forth along the x axis. During the measurement, the slow scan in the y direction is disabled. The load is gradually decreased from the top to the bottom along the y axis until the tip snaps out of contact (marked by a dashed line in the figure). Figure 2(b) shows the change in the friction force with load from these experiments, wherein each data point is an average of 256 friction line loops. The continuous lines are fits to the Derjaguin-Müller-Toporov (DMT) and Johnson-Kendall-Roberts (JKR) continuum elastic contact models assuming proportionality between friction force and contact area, $F = \tau \cdot A$, with the shear strength, $\tau = 46.5\,GPa$, the only fitting parameter.[23,24] As can be seen from the figure, the agreement of the numerical fit based on the DMT model to experimental data is excellent.[25,26] At the maximum total load of 24 nN, the contact area is estimated to be 19 nm^2 based on the DMT model, corresponding to an average pressure of 1.26 GPa, which is well below the yield strength of bulk GaAs and Pt.[27,28] The absence of irreversible deformation was also confirmed by AFM scanning over the same surface region after the friction measurement.

Band bending occurs when a voltage is applied between the AFM tip and GaAs sample. Figure 3(a) shows the energy band diagram of the tip-oxide-semiconductor junction for sample biases of +1.5V and -1.5V. At the sample bias of -1.5V, the conduction band edge moves upward in energy and may cross the Fermi level near the surface.[29] Since the carrier density is exponentially dependent on the energy difference between the Fermi level and conduction band edge, this band bending causes accumulation of majority carriers (electrons for an n-type sample) near the semiconducting surface. At the sample bias of +1.5V, the bands bend downward and carriers are depleted away from the surface or under weak inversion. This rectifying effect is clearly observed in the current-voltage characteristics, which are shown in Figure 3(b), wherein the current is due to electrons tunneling through the thin oxide layer.[30]

Figure 4 shows (a) current, and (b) friction images when the sample bias was changed from +2.5V to -2.5V and back to +2.5V on three successive scanning regions. Figure 4(c) is an averaged line profile of Figs. 4(a) and 4(b). At -2.5V, the sample is forward biased and in strong accumulation, leading to a high carrier concentration near the surface. At +2.5V, the sample is reverse biased, causing depletion or weak inversion. As a result, the current tunneling through the oxide layer was high at the -2.5V bias (4 nA) and low at the +2.5V bias (0.1 nA), as shown in Fig. 4(c). As can be seen, friction is $\sim$ 20% higher when the sample is forward biased.

Besides varying the carrier density, another effect of the bias voltage is that the electrostatic force increases the effective load on the sample, leading to an increased friction force. This effect can be quantitatively evaluated by measuring the change in the tip-sample pull-off force as a function of the bias voltage, as shown in Figure 5. Each data point is an average of 5 independent measurements and the error bar is associated with the standard deviation of the measurements. As shown in Figure 5, the electrostatic contribution to the pull-off force approximately follows a parabolic law, i.e., $F_{elec} \propto V^2$, with the minimum at $V_c = -0.46V$ due to the contact potential difference between the tip and the substrate. To exclude the small effect of the non-zero contact potential difference on friction, we define an effective sample bias as $V_e = V_s - V_c$, so that the electrostatic forces at $\pm V_e$ are equal.

In the case of GaAs, the electrostatic field from the tip can induce band bending, which can significantly change the carrier distribution near the surface. One would think that the asymmetric charge distribution could give rise to the asymmetric behavior of the pull-off

force between accumulation and depletion. The GaAs substrate reaches inversion at a reverse bias larger than $+1.4V$.[31] For a semiconductor under inversion, similar to accumulation, incremental charges are added or subtracted at the GaAs/oxide interface, leading to a similar electrostatic contribution to the pull-off force. For a bias between 0 and $+1.4V$, the sample is in depletion, with a maximum depletion width of $40\,nm$ at a reverse sample bias of $+1.4V$.[32] Experimentally, we do not observe a significant deviation from a quadratic dependence of the pull-off force changes on bias (Figure 5). For $-1.4V < V_e < +1.4V$ (around the bottom of the parabola), the variation in the pull-off force is less than 5nN, which only causes little change to friction force. To quantify the effect of the asymmetric charge distribution when $-1.4V < V_e < +1.4V$, a three dimensional model taking into account band bending would be necessary, which is out of the scope of this paper. In addition, the data we present are either in the accumulation or inversion regimes, wherein this effect is only a minor contribution.

Figure 6(a) shows a plot of the friction force versus load at the sample biases of $V_e = +2V$ and $-2V$. A clear enhancement in the friction force at a forward bias is visible as compared to that at a reverse bias. The negative loads shown on the x axis reflect the adhesion contribution that keeps the tip against the surface even when the cantilever applies a tensile stress to the tip-sample contact. The line through the friction data in Fig. 6 is a DMT fit. While the agreement with the DMT curve is very good at a reverse bias, at a forward bias, it shows a significant "excess" friction. The excess friction is found to be proportional to (total load)$^{\alpha}$, where α is approximately 1.5. Figure 6(b) shows a plot of the current versus load at the sample biases of $V_e = +2V$ and $-2V$. At the sample bias of $V_e = +2V$, the sample is reverse biased, and the current is below $5\,pA$ for the range of load used in the experiment. When the sample is forward biased at $V_e = -2V$, the current approximately exponentially increases with respect to the applied load. The exponential increase in current versus load suggests a decrease in the oxide tunneling barrier thickness as a result of the pressure exerted by the tip. The relationship between the current and contact area was addressed earlier on boron doped hydrogen terminated diamond (111) and on Si surfaces.[24,33] These studies reveal a proportionality between the current and contact area. In our experiment on GaAs, the elastic deformation of the oxide layer at the tip/sample contact results in a departure from the previously observed linear relationship between the current and contact area.

Figure 7 shows plots of friction versus effective sample bias V_e at an external load of $+5nN$. Each data point is an average of 256 friction loops. As can be seen, excess friction

is apparent for biases more negative than $-1.25V$. The continuous line shows the predicted parabolic increase in friction calculated from the change in the electrostatic force. The increase in friction with bias in the reverse bias region is purely the result of the increase in the electrostatic force.

Figure 8 shows the velocity dependence of the friction force. At the reverse bias (+1.5V), the friction only slightly increases with scanning speed, while under the forward bias (-1.5V), it shows a larger and approximately linear dependence on velocity.

It should be noted that the data in Figs. 2 and 4-8 were obtained with different tips. Although an absolute comparison is difficult, the trends in the figures are consistent.

IV. DISCUSSION

We can compare the excess friction observed in our experiments with experimental and theoretical investigations on electronic contributions to friction in other systems. Persson and Tosatti[1,2] analyzed the electronic dissipation (friction) in many systems. In most systems, the electronic dissipation is proportional to the velocity, so $F_e = \Gamma_{el} v$, where v is the velocity and Γ_{el} is a dissipation parameter characteristic of the system.

We observed $0.04nN$ of additional friction force for tip-sample velocities of $8\mu m/s$ at an effective sample bias of $-1.5V$ and at a load of $1.5nN$, as shown in Fig. 8, leading to an experimental dissipation Γ_{expt} of $5 \times 10^{-6} Ns/m$. In our earlier study[10] on silicon pn junctions, the p stripes were doped to $5 \times 10^{18}/cm^3$. Excess friction observed in p regions at a bias of +4V and a load of 8nN leads to a dissipation Γ_{tip} of $2 \times 10^{-5} Ns/m$.

Frictional dissipation in metallic and semiconductor surfaces was recently investigated in experiments by using a lever perpendicular to the surface.[34–36] Stipe et al.[35] observed dissipation when a gold tip moved parallel to a gold surface without touching. The dissipation approximately increased as the inverse of the tip-sample distance and as the square of the bias. At room temperature and near-zero bias, they observed a dissipation of $\Gamma_{tip} \sim 10^{-12} Ns/m$ at 2.5 nm from the surface. Such dissipation was interpreted in terms of near-surface fluctuating electric fields interacting with the static surface charge by using the fluctuation-dissipation theorem. Dorofeyev et al.[34] measured the tip-sample dissipation through observation of thermal fluctuations for an Al-coated tip moving perpendicular to a gold surface, obtaining a tip-sample dissipation of $\Gamma_{tip} \sim 4 \times 10^{-9} Ns/m$ for a near-zero bias, which they attributed

to the non-conservative Joule loss of the induced image current due to electromagnetic fields originated from the thermal fluctuation of the cantilever. Volokitin and Persson[36] have theoretically analyzed dissipation for a metallic tip moving close to a surface. For clean conductors and a parabolic tip apex, they estimated an upper limit to the electronic friction of the tip, which is $< 10^{-15} Ns/m$; however, in the presence of adsorbates that can vibrate with acoustical modes parallel to the surface, this value increased to $7 \times 10^{-13} Ns/m$. The authors attributed such an enhancement to the Van der Waals friction increase in the case of a resonant photon tunneling between low-frequency surface plasmon modes and adsorbate vibrational modes. Denk and Pohl[37] estimated Joule dissipation associated with dragging carrier charges to be below $10^{-11} Ns/m$. Kuehn et al.[38,39] performed experiments measuring non-contact dissipation on polymer films on Au. The observed dissipation was attributed to dielectric fluctuations that were modeled by using the fluctuation-dissipation theorem. Extrapolation of the values of Kuehn et al.[38,39] to our parameter values ($V = 2 \sim 4V$; d = 1 nm) by using their finding that Γ approximately varies as V^2/d, leads to Γ of $10^{-8} \sim 10^{-9} Ns/m$, which is 3 orders of magnitude smaller than our measured value.

We now estimate Ohmic losses from the charge accumulated under the tip region under a forward bias in our experiments. From four-point probe measurements, the resistivity of the GaAs substrate is $\rho = 2.1 \times 10^{-3} \Omega cm$. Based on the Drude model, by assuming that electrons are back-scattered for every period of time equal to the relaxation time t, the dissipation per electron is $\Gamma_2 = F_e/v = (2mv/t)/v = 2m/t$. The relaxation time can be computed for a metal or semiconductor from the expression $t = m/(ne^2\rho)$.[40] So, the dissipation per electron is $\Gamma_e = 2m \cdot ne^2\rho/m = 2ne^2\rho = 1.3 \times 10^{-18} Ns/m$, where the donor concentration $n = 1.2 \times 10^{18}/cm^3$. By using an oxide thickness of $t_{ox} = 1nm$ (determined by XPS) and the dielectric constant of the GaAs oxide of $\epsilon_{ox} = 10$,[41] the capacitance per unit area between the Pt tip and GaAs substrate is $C_{ox} = \epsilon_0 \epsilon_{ox}/t_{ox} = 0.09\, F/m^2$. Under the forward bias of $V_e = -1.5V$, the accumulated charge density is $Q_{acc} = C_{ox} V_e = 0.13\, C/m^2$. The mechanical contact area at a load of 3.5nN is $5.3\, nm^2$. The number of accumulation charge in the contact area (at the bias of 1.5V) is then $n_0 = Q_{acc} A/e = 4.4$. This gives a dissipation due to Ohmic loss of $\Gamma_{ohmic} = n_0 \Gamma_e = 3.8 \times 10^{-18} Ns/m$. This value is 12 orders of magnitude lower than the experimental result.

The tip-sample force deforms the GaAs lattice. This has two possible effects, which are strain-induced band bending and stress-induced carrier scattering.[42] We estimated the upper

limit of the stress-induced carrier scattering, $\Gamma_{stress} < 6 \times 10^{-20} Ns/m$.[43] This is 14 orders of magnitude lower than our observed value. The semiconductor band gap can change under strain in the gigapascal range. It was proposed that the formation of a pressure induced quantum dot under the tip could enhance electron-hole recombination, with the energy emitted in the form of phonons or photons.[9,10] In contrast to silicon *pn* junction experiments,[9,10] for GaAs, the conduction band edge moves up in energy under hydrostatic pressures[44,45] leading to repulsion of the electrons away from the tip-sample contact region. This decreases the effect of the electron-hole pair recombination rate and is inconsistent with our observation of increasing excess friction versus applied load [Figure 6(a)].

It is clear, therefore, that our observed excess friction in accumulation cannot be due to any of these mechanisms because it is several orders of magnitude higher.

A possible mechanism is electrostatic effects from trap states in the oxide layer populated by electrons under the applied electric field. In accumulation the potential drop in GaAs is negligible. Almost all the sample bias is applied to the oxide, resulting in a linear potential drop in the oxide. The large field and/or tunneling electrons can populate the trap states. At the reverse bias, the tunneling current is 40 times smaller and the potential drop in the depletion region reduces the field in the oxide, making population of the trap states less likely. As the tip moves across the sample surface, it leaves a "trail" of charged traps, causing an additional electrostatic attraction to the tip, which shows up as friction. Based on the DMT model, the mechanical contact area at a load of 3.5nN is $5.3\,nm^2$. At the GaAs/oxide interface the trap state areal density (including bulk and interface traps) is on the order of $1 \times 10^{13}/cm^2$.[29,46] The diameter of the contact area is $d = \sqrt{4A/\pi} = 2.6\,nm$. There are 0.5 traps in the contact area, leading to $\sigma = 0.5/d = 0.2$ trap every nanometer along the scan direction. The lifetime of trap states in GaAs ranges from $10\,ms$ to $1\,\mu s$ depending on the energy position inside the gap.[47] The lifetime for the trap states in an oxide can be even longer because of the wider energy band gap. Let us assume that the lifetime of trap states in GaAs oxide is $\tau \sim 1\,ms$, which is comparable to the lifetime reported in a recent study on Ga_2O_3 nanowires.[48] With a scanning velocity of $v = 8\,\mu m/s$, the length of the scanning pathway with charged (non-relaxed) trap states is of the order of $L = v\tau = 8\,nm$. The total number of nonrelaxed traps is $n_1 = 1.6$. The negative trapped charges induce positive image charges on the tip, causing an attractive force between the tip and the trapped charges. In addition, a forward bias (negative sample voltage) also causes the tip to have positive

charges, which adds to the attraction between the tip and sample. As we calculated in the case of Ohmic loss, the number of accumulation charge in the contact area (at the bias of 1.5V) is $n_0 = Q_{acc}A/e = 4.4$. The total charge on the Pt tip is the sum of the image charge and the accumulated charge, $n = n_0 + n_1 = 6$. By assuming that the trap states are located in the middle of the oxide, which leads to a vertical distance between the charges on the tip and the trapped charges in the oxide to be $l = 1\,nm$, the excess friction force needed to compensate the electrostatic attraction between the charged traps and the charges on the tip is $F_{trap} = \int_0^L ne\sigma e/[4\pi\epsilon_0\epsilon_{ox}(x^2 + l^2)]x/\sqrt{x^2 + l^2}\,dx = 0.03\,nN$, which is within a factor of 2 of the experimental value (Fig. 8).

As the velocity increases, the pathway containing non-relaxed traps and the total image charges on the tip would increase, which is consistent with our data, as shown in Figure 8. Our model of charged trap states also explains the existence of a threshold bias for the observation of excess friction. This threshold bias voltage is needed to initiate the population of trap states, and the population will then increase with bias voltage, resulting in an increase in the excess friction. This effect is consistent with the experimental observation of an increase in excess friction as a function of the bias voltage (Fig. 7).

Another interesting experiment is changing the density of charged trap states by varying the oxide thickness and testing its influences on friction forces.

V. CONCLUSION

In conclusion, by using an n-type GaAs (100) substrate with a net donor concentration of $1.2 \times 10^{18}/cm^3$, we have shown that electronic effects in the nanoscale friction properties can be significant. By varying the bias between the tip and the sample, charge depletion or accumulation could be induced, which results in significant differences in the friction force. The observation of an excess friction at the forward bias on n-GaAs, together with a previously reported observation on p-Si, suggests that electronic contribution to friction is a general effect. We have also reviewed many possible sources of electronic contribution to friction, including electron-hole pair creation, electron wind, charge carrier dragging, and fluctuation electric fields. In all cases, we have shown that under our conditions, these contributions are too small to explain our observations. A more likely model was been proposed based on electrostatic effects arising from charges trapped in near-surface layers

located either in the semiconductor or in the oxide gap. These states are charged in the forward bias and produce electrostatic forces on the tip of the correct magnitude. The model also explains reasonably well the observed velocity dependence. Our observations indicate that the electric field can be used to control the friction on semiconductors covered with a thin oxide layer, offering an interesting way of tuning or switching the frictional response in nanoscale devices.

VI. ACKNOWLEDGMENT

This work was supported by the Director, Office of Science, Office of Basic Energy Sciences, Materials Sciences and Engineering Division, of the U.S. Department of Energy under Contract No. DE-AC02-05CH11231.

---

[1] B. N. J. Persson and E. Tosatti, *Physics of Sliding Friction* (Springer-Verlag, New York, 1996).

[2] B. N. J. Persson, *Sliding Friction: Physical Principles and Applications* (Springer-Verlag, Berlin, 1998).

[3] R. Carpick and M. Salmeron, Chem. Rev. **97**, 1163 (1997).

[4] E. Gnecco, R. Bennewitz, T. Gyalog, and E. Meyer, J. Phys. Condens. Matt. **13**, R619 (2001).

[5] R. Cannara, M. Brukman, K. Cimatu, A. Sumant, S. Baldelli, and R. Carpick, Science **318**, 780 (2007).

[6] A. Dayo, W. Alnasrallah, and J. Krim, Phys. Rev. Lett. **80**, 1690 (1998).

[7] G. Witte, K. Weiss, P. Jakob, J. Braun, K. L. Kostov, and C. Woll, Phys. Rev. Lett. **80**, 121 (1998).

[8] M. Highland and J. Krim, Phys. Rev. Lett. **96**, 226107 (2006).

[9] J. Y. Park, D. F. Ogletree, P. A. Thiel, and M. Salmeron, Science **313**, 186 (2006).

[10] J. Y. Park, Y. Qi, D. F. Ogletree, P. A. Thiel, and M. Salmeron, Phys. Rev. B **76**, 064108 (2007).

[11] M. G. Kang, S. H. Sa, H. H. Park, K. S. Suh, and K. H. Oh, Thin Solid Films **308-309**, 634 (1997).

[12] C. Thurmond, G. Schwartz, G. Kammlott, and B. Schwartz, J. Electrochem. Soc. **127**, 1366

(1980).

[13] J. Y. Park, D. F. Ogletree, M. Salmeron, R. A. Ribeiro, P. C. Canfield, C. J. Jenks, and P. A. Thiel, Phys. Rev. B **74**, 024203 (2006).

[14] M. R. Vilar, J. E. Beghdadi, F. Debontridder, R. Artzi, R. Naaman, A. M. Ferraria, and A. M. B. do Rego, Surf. Interface Anal. **37**, 673 (2005).

[15] RHK Technology, Troy, MI USA, model No: UHV-350.

[16] J. Y. Park, D. F. Ogletree, M. Salmeron, C. J. Jenks, and P. A. Thiel, Tribol. Lett. **17**, 629 (2004).

[17] J. Y. Park, D. F. Ogletree, M. Salmeron, R. A. Ribeiro, P. C. Canfield, C. J. Jenks, and P. A. Thiel, Phys. Rev. B **71**, 144203 (2005).

[18] E. Sahagún, P. García-Mochales, G. M. Sacha, and J. J. Sáenz, Phys. Rev. Lett. **98**, 176106 (2007).

[19] S. Jian, T. Fang, and D. Chuu, J. Phys. D: Appl. Phys. **38**, 2424 (2005).

[20] NanoAndMore USA Co., Beaufort, SC USA.

[21] J. Sader, J. Chon, and P. Mulvaney, Rev. Sci. Instrum. **70**, 3967 (1999).

[22] D. F. Ogletree, R. W. Carpick, and M. Salmeron, Rev. Sci. Instrum. **67**, 3298 (1996).

[23] F. P. Bowden and D. Tabor, *The Friction and Lubrication of Solids* (Oxford University Press, Oxford, 1950).

[24] M. Enachescu, R. van den Oetelaar, R. Carpick, D. Ogletree, C. Flipse, and M. Salmeron, Phys. Rev. Lett. **81**, 1877 (1998).

[25] D. Maugis, J. Colloid Interface Sci. **150**, 243 (1992).

[26] R. Carpick, D. Ogletree, and M. Salmeron, J. Colloid Interface Sci. **211**, 395 (1999).

[27] E. L. Bourhis and G. Patriarche, Mater. Sci. Eng. A **309-310**, 478 (2001).

[28] A. Kavner and T. S. Duffy, Phys. Rev. B **68**, 144101 (2003).

[29] S. M. Sze, *Physics of Semiconductor Devices* (Wiley, New York, 1981).

[30] A possible effect of the current is to increase the temperature at the contact. Since Pt is much more electrically conductive than GaAs, we expect that the Joule heat is mostly generated on the sample side. A simple two dimensional thermal transport calculation shows a temperature increase of $\sim 2\,^{\circ}C$ by using a thermal conductivity of $0.55\,W cm^{-1}K^{-1}$), a current of $2\,\mu A$, a sample bias of 3V, and a contact radius of $10\,nm$.

[31] The intrinsic carrier density in GaAs at room temperature is $n_i = 10^7/cm^3$ (Ref.[49]). The

difference between the middle of the band gap and the Fermi level of GaAs with a doping concentration of $N_D = 1.2 \times 10^{18}/cm^3$ is $\psi_f = kT \cdot ln(N_D/n_i)/e = 0.66\,V$. When the GaAs substrate reaches inversion, the potential drop in semiconductor is $\psi_s = 2\psi_f = 1.32V$. The dielectric constant of GaAs is $\epsilon_{GaAs} = 13.2$ (Ref.[29]). The dielectric constant of the GaAs oxide is $\epsilon_{ox} = 10$ (Ref.[41]). The voltage drop over the oxide of thickness $1\,nm$ is $V_{ox} = \sqrt{2qN_D\epsilon_0\epsilon_{GaAs}\psi_s}t_{ox}/\epsilon_0\epsilon_{ox} = 0.09\,V$ (Ref.[29]). So the critical bias voltage for the GaAs substrate to change from depletion to inversion is $1.41\,V$.

[32] The maximum width of the depletion region is $W_{Dm} = \sqrt{2\epsilon_0\epsilon_{GaAs}\psi_s/(qN_D)} = 40\,nm$ (Ref.[29]).

[33] J. Y. Park, R. J. Phaneuf, D. F. Ogletree, and M. Salmeron, Appl. Phys. Lett. **86**, 172105 (2005).

[34] I. Dorofeyev, H. Fuchs, G. Wenning, and B. Gotsmann, Phys. Rev. Lett. **83**, 2402 (1999).

[35] B. C. Stipe, H. J. Mamin, T. D. Stowe, T. W. Kenny, and D. Rugar, Phys. Rev. Lett. **87**, 096801 (2001).

[36] A. I. Volokitin and B. N. J. Persson, Surf. Sci. **587**, 88 (2005).

[37] W. Denk and D. W. Pohl, Appl. Phys. Lett. **59**, 2171 (1991).

[38] S. Kuehn, R. F. Loring, and J. Marohn, Phys. Rev. Lett. **96**, 156103 (2006).

[39] S. Kuehn, J. A. Marohn, and R. F. Loring, J. Phys. Chem. B **110**, 14525 (2006).

[40] N. W. Ashcroft and N. D. Mermin, *Solid State Physics* (Saunders, Philadelphia, 1976).

[41] M. Passlack, N. E. J. Hunt, E. F. Schubert, G. J. Zydzik, M. Hong, J. P. Mannaerts, R. L. Opila, and R. J. Fischer, Appl. Phys. Lett. **64**, 2715 (1994).

[42] S. S. Li, *Semiconductor Physical Electronics* (Plenum, New York, 1993).

[43] The Fermi velocity of electrons in GaAs is $v_{Fermi} \sim 3 \times 10^7\,cm/s$ (Ref.[50]). The effective electron mass in GaAs is $m_n = 0.09m_e$ (Ref.[51]), where $m_e = 9.1 \times 10^{-31}kg$ is the electron rest mass.

[44] M. Boucenna and N. Bouarissa, Mater. Chem. Phys. **84**, 375 (2004).

[45] S. Saib and N. Bouarissa, Solid-State Electron. **50**, 763 (2006).

[46] A. Kapila and V. Malhotra, Optoelectronic and Microelectronic Materials and Devices Proceedings, 1996 Conference on pp. 275–282 (1996).

[47] G. Brammertz, K. Martens, S. Sioncke, A. Delabie, M. Caymax, M. Meuris, and M. Heyns, Appl. Phys. Lett. **91**, 133510 (2007).

[48] Y. P. Song, H. Z. Zhang, C. Lin, Y. W. Zhu, G. H. Li, F. H. Yang, and D. P. Yu, Phys. Rev. B **69**, 075304 (2004).

[49] C. Gooch, C. Hilsum, and B. Holeman, J. Appl. Phys. **32**, 2069 (1961).

[50] D. K. Ferry and S. M. Goodnick, *Transport in Nanostructures* (Cambridge University Press, Cambridge, UK, 1997).

[51] V. A. Bogdanova, N. A. Davletkildeev, N. A. Semikolenova, and E. N. Sidorov, Semiconductors **36**, 385 (2002).

List of Figures

Figures

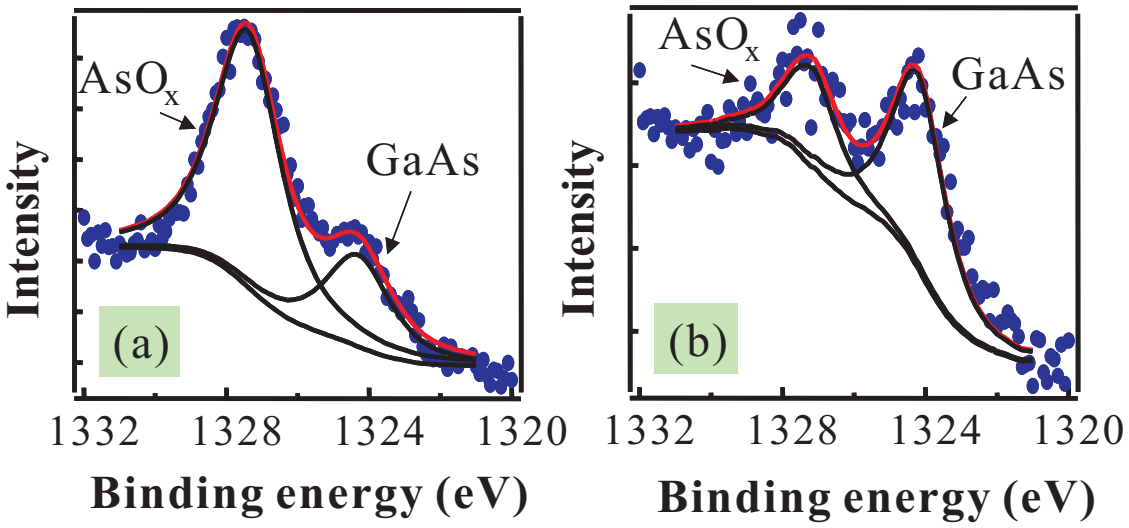

FIG. 1: (Color online) XPS 2p spectral region of arsenic (a) before and (b) after etching and reforming the oxide.

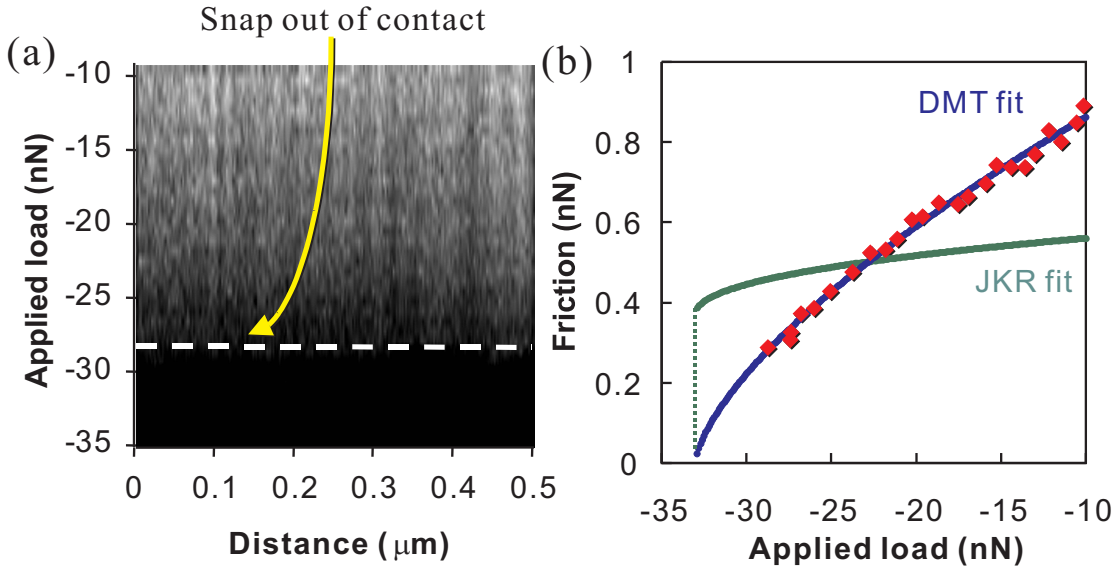

FIG. 2: (Color online) (a) Friction map as a function of applied load at 0V sample bias (scanning speed=500nm/s). (b) Plot of the friction force versus load at 0V sample bias.

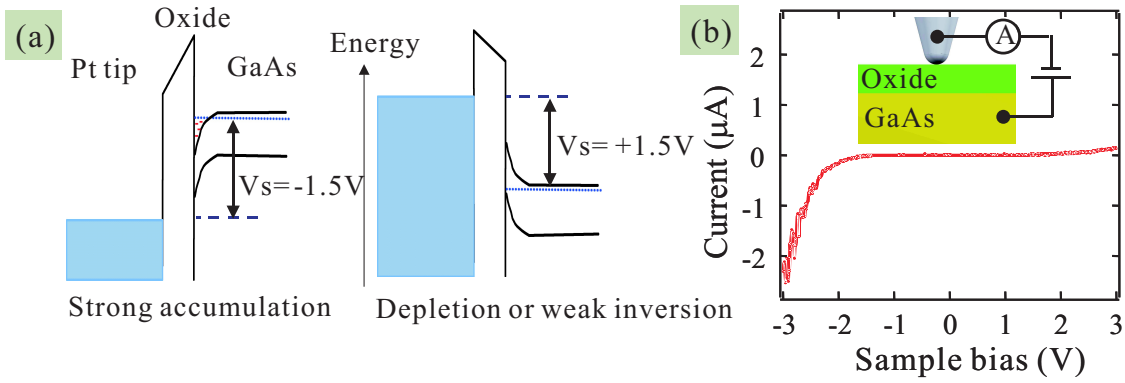

FIG. 3: (Color online) (a) Schematic illustration of the band structure of the tip-oxide-semiconductor junctions for sample biases of -1.5V and +1.5V. (b) Plot of current versus sample bias at a total load of 36nN.

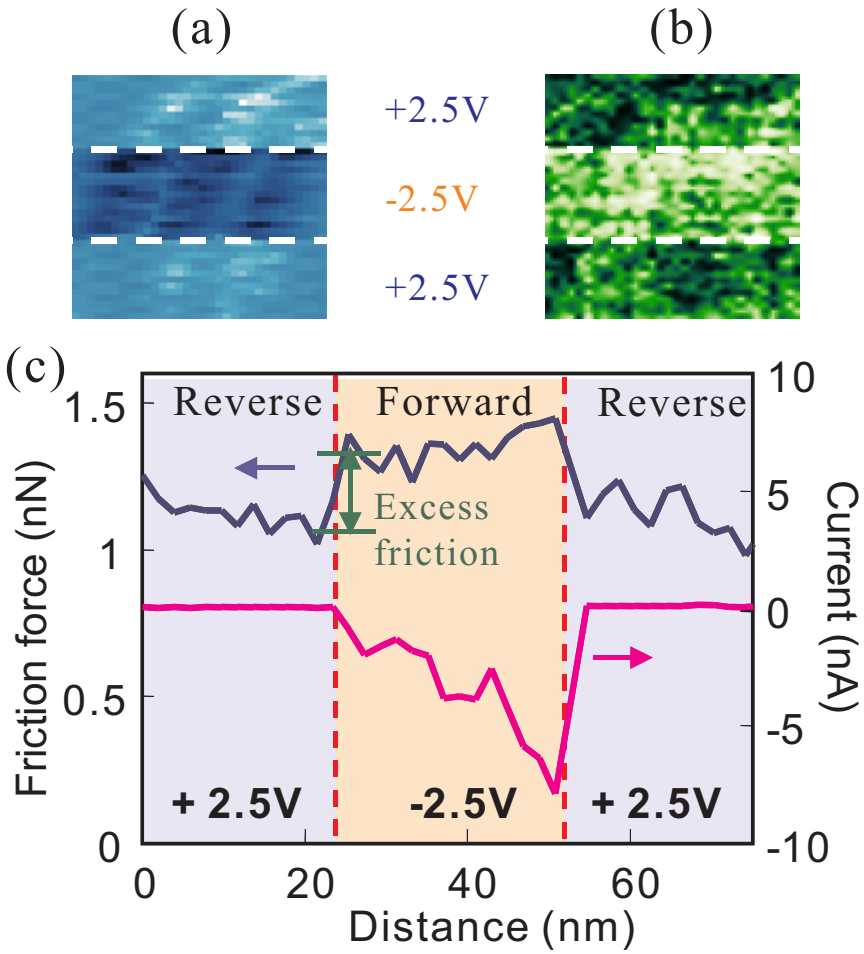

FIG. 4: (Color online) (a) $75 \times 75\, nm^2$ current, and (b) friction images with sample biases of +2.5V and -2.5V (scanning speed=$1\mu m/s$ and total load=8nN). The dashed lines mark the positions where the changes in the bias voltage are made. (c) Averaged line profiles of the vertical cross sections in the current image shown in (a) and in the friction image shown in (b).

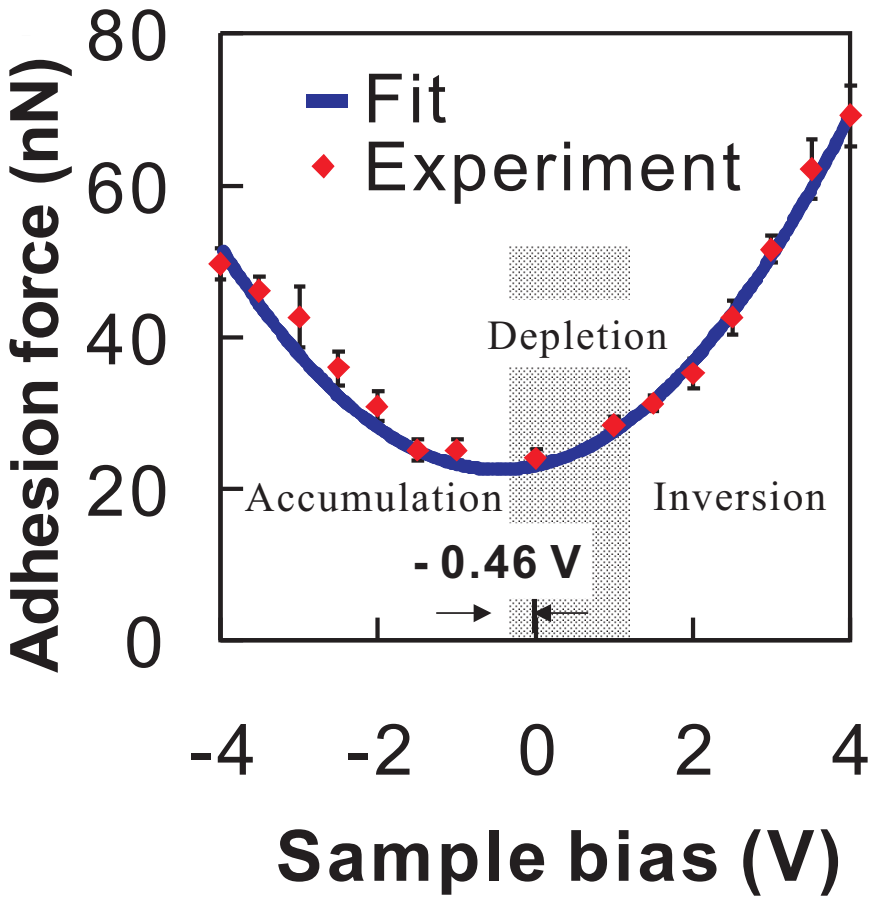

FIG. 5: (Color online) Plot of the pull-off force as a function of sample bias. The error scales represent the standard deviation from five measurements. A fit to a parabolic function is shown by the continuous line. The center of the parabola is at -0.46 V, reflecting the contact potential difference between the tip and the surface.

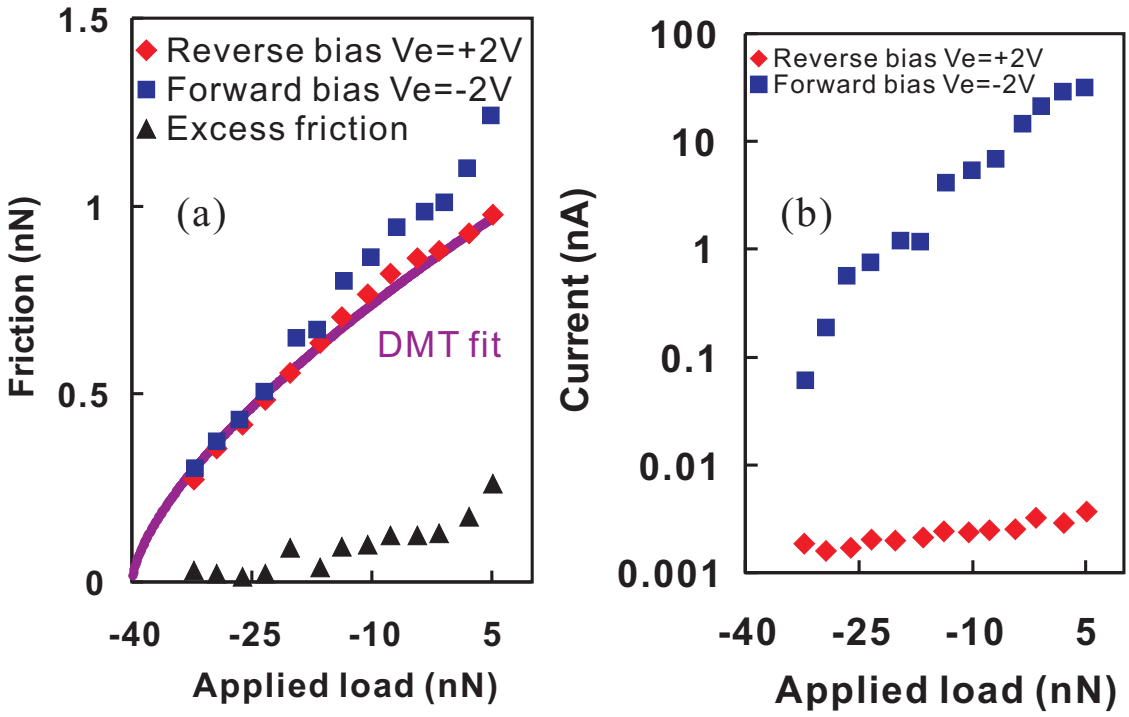

FIG. 6: (Color online) (a) Plot of the friction force and (b) the current versus load at effective sample biases of +2V and -2V at a scanning speed of 500nm/s.

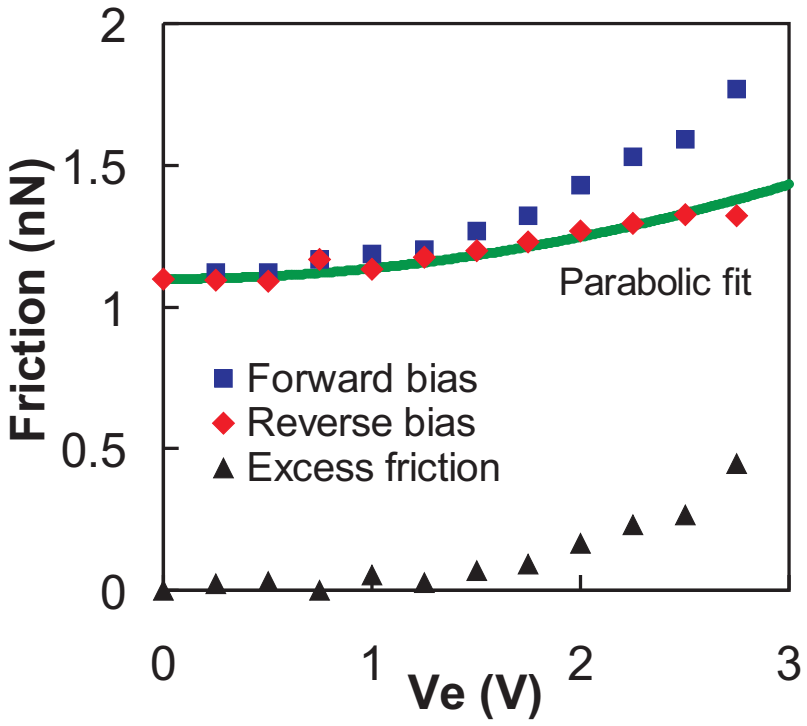

FIG. 7: (Color online) Friction force as a function of sample bias (total load=5nN and scanning speed= 500nm/s). As the voltage increases, the load increases too due to the electrostatic contribution ($\propto V_e^2$) in both polarities.

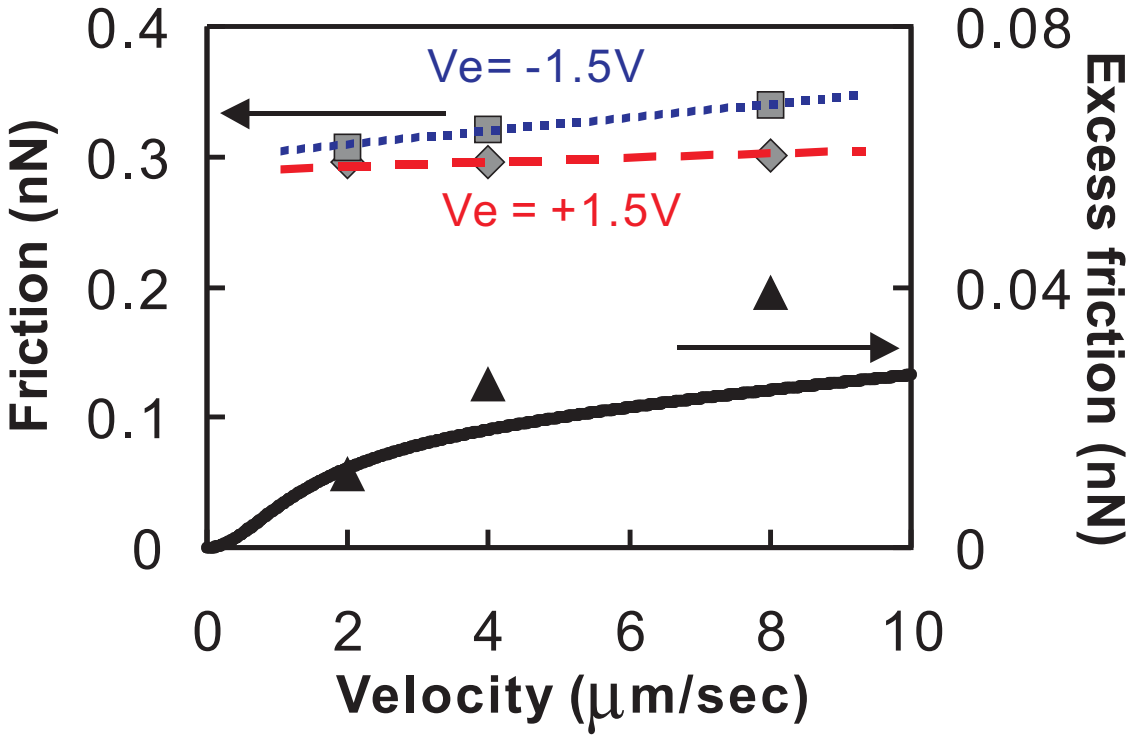

FIG. 8: (Color online) Friction force as a function of scanning speed (load =3.5 nN) at sample biases of V_e = -1.5V (square) and +1.5V (diamond). The lines are drawn to highlight the trends in the data. The difference or excess friction increases with the sliding velocity (triangles). The solid curve is calculated based on the electrostatic contribution from the charged trap states in the oxide.